Mechanism and Machine Theory 73 (2014) 103–116

Contents lists available at ScienceDirect

Mechanism and Machine Theory

journal homepage: www.elsevier.com/locate/mechmt

Design and development of a hand exoskeleton for rehabilitation of hand injuries

Fuhai Zhang *, Lei Hua, Yili Fu, Hongwei Chen, Shuguo Wang

State Key Laboratory of Robotics and System, Harbin Institute of Technology, 150001 Harbin, China

ARTICLE INFO

Article history:
Received 13 October 2012
Received in revised form 25 October 2013
Accepted 29 October 2013
Available online 28 November 2013

Keywords:
Rehabilitation
Hand exoskeleton
Circuitous joint
Bowden cable

ABSTRACT

Hand injuries are common problems. In order to adapt to fingers of different sizes and avoid secondary injuries, a hand exoskeleton for rehabilitation is proposed. The exoskeleton is designed as a wearable device and each finger has three joints named the metacarpophalangeal (MCP) joint, the proximal interphalangeal (PIP) joint and the distal interphalangeal (DIP) joint which all employ a novel mechanism called "circuitous joint". Adopting a symmetrical pinion and rack with a parallel sliding mechanism, the circuitous joint can cover a wide workspace of the finger and adapt to fingers of different thicknesses. And the parallel sliding mechanism ensures that the contact force between the exoskeleton and the finger is perpendicular to the finger's bone, which can minimize the secondary injuries. Moreover, the Bowden cable driving method reduces the burden on the fingers by placing the driving and control system on the forearm. Lastly, hand fitness test and contact force experiment are conducted and the results verify the rationality and effectiveness of the exoskeleton.

1. Introduction

Hand is one of the most important organs of human body, and its normal motor capability is crucial for people's daily activities. However, hand injuries are common problems, especially in occupational accidents. These injuries can lead to a loss of sensation and motor functions of the hand. It is essential to perform rehabilitation for the hand to regain previous dexterity. Currently most rehabilitation activities are performed manually by physiotherapists. However, it causes high personnel costs and the lack of motivation of patients to perform exercises.

Recent researches showed that exoskeleton devices based on rehabilitation theory are feasible and effective [1,2]. However, most existing exoskeleton devices were not developed for rehabilitation purposes. Some exoskeleton devices were designed for master–slave systems [3–5], and some were designed as the force feedback devices [6]. They are limited in the number of independently actuated degrees of freedom and may cause secondary injuries easily. Nevertheless, research on hand exoskeletons has already achieved promising results. The exoskeleton designed at the Technical University of Berlin [7,8] has 4 DOFs (degrees of freedom) and can actuate each finger joint by the linkage mechanism, but additional changeable attachments are needed to fit different hand sizes. Worsnopp et al. [9] proposed a virtual prototype with 3 DOFs which can only be assembled on the lateral side of the finger, so it cannot be applied to the middle and ring fingers. Yamaura [10] proposed a hand rehabilitation device that is adjustable to accommodate various hand sizes but only has two DOFs for each finger. An exoskeleton with four DOFs was developed which can realize the passive rehabilitative training [11]. In addition, the exoskeleton designed by Wang for index finger rehabilitation [12,13] can realize multiple rehabilitation motions, but the huge driving system is a

Abbreviations: MCP, metacarpophalangeal; PIP, proximal interphalangeal; DIP, distal interphalaneal; DOF, degrees of freedom; SPRM, symmetrical pinion and rack mechanism

* Corresponding author at: State Key Laboratory of Robotics and System, Harbin Institute of Technology, Harbin, Heilongjiang Province, China. Tel./fax: +86 45186403219.
E-mail address: fuzh_hit@163.com (F. Zhang).

0094-114X/$ – see front matter © 2013 Elsevier Ltd. All rights reserved.
http://dx.doi.org/10.1016/j.mechmachtheory.2013.10.015

conspicuous problem. Due to the special medical application, there are many unsolved issues and the design of exoskeletons is still an investigation field full of challenges. Most of the devices introduced above can't accommodate a variety of hand sizes. Also contact forces between the exoskeleton and fingers aren't always perpendicular to the bones of the fingers during the rehabilitation process, which causes secondary injuries easily. Fu et al. [14] preliminarily discussed the feasibility to solve the above problems by designing a "circuitous joint" which can stretch and rotate at the same time, and put forward the design scheme of the hand exoskeleton. It is composed of the adaptive dorsal finger exoskeleton, the adaptive dorsal metacarpal base and the Bowden cable driven actuator, and the initial 3D model is established in Pro/E.

In this paper, we design and manufacture a novel hand exoskeleton. Our exoskeleton is designed specifically for the actual requirements of rehabilitation applications for injured fingers. We first finish the fully detailed mechanical design of the device, especially perfect the optimal structure design of the "circuitous joint"; by employing the "circuitous joint", our exoskeleton can cover a wide workspace of a finger and adapt to a variety of fingers with different thicknesses. Second, we introduce the driving method and contact force analysis. Bowden cable driving is recommended and it can actuate each joint bilaterally and reduce the burden on the fingers. Lastly the hand fitness test and contact force experiment are conducted.

2. Mechanical design of the hand exoskeleton

Our novel hand exoskeleton conception for rehabilitation, shown in Fig. 1, is designed as a wearable device. The device is composed of two main parts: the adaptive exoskeleton and the Bowden cable driving actuator. The exoskeleton includes the metacarpophalangeal (MCP) joint, the proximal interphalangeal (PIP) joint and the distal interphalaneal (DIP) joint. The Bowden cable driven actuator with two cables can actuate each joint bilaterally. Next we will introduce the mechanical design of the hand exoskeleton.

2.1. Fundamental design of the circuitous joint

Recently some dexterous robot hands have been developed. These hands can be divided into two categories. One is endoskeleton type. Although it is light-weight and compact, it does not allow complete fist closure because of the placement of the actuators in the palm [15]. The other is exoskeleton type which most of the robot hands adopt. When designing such an exoskeleton, the main theme is focused on the joint mechanisms. The most practical joint is a revolute one that consists of an axis and bearings, and the general way to place it corresponding to an operator's joint is in parallel on backside or in coaxial beside. However, the former tends to narrow the movable range of the operator's joint [4] and the latter cannot find existing space between the operator's fingers [9]. Furthermore, interesting mechanisms [16] are developed, but the problem on how to accommodate to a variety of fingers is still unsolved.

Through observation we discover that the hand exoskeleton should have a stretching displacement along the finger when it actuates a finger in order to solve the issue mentioned above. Therefore this paper proposes a novel joint mechanism named "circuitous joint", which adopts the symmetrical pinion and rack mechanism (hereinafter called "the SPRM"). The fundamental mechanism is shown in Fig. 2. A gear rotates on a rack by relative rotation of two segments, and the shifting of its axis provides stretching of a segment that has the rack. Since the two segments should make same stretching displacement together, two sets of the mechanisms are combined in the opposite direction. Thus two segments have a stretching displacement when a gear has a rotation on the corresponding rack.

However, it is obvious that the stretching displacement S produced by the SPRM is always keeping in proportion to the angular displacement θ. The relationship between the angular displacement θ and the stretching displacement S must be non-linear to cover wide workspace of the finger and the stretching displacement required for different fingers is different. For this reason, a parallel sliding mechanism is adopted. The SPRM is placed in two slots which are fixed on the finger. Segment A and segment B can slide passively along the slots. Thus an extra extension displacement S_1 is obtained by the mechanism itself when stretching

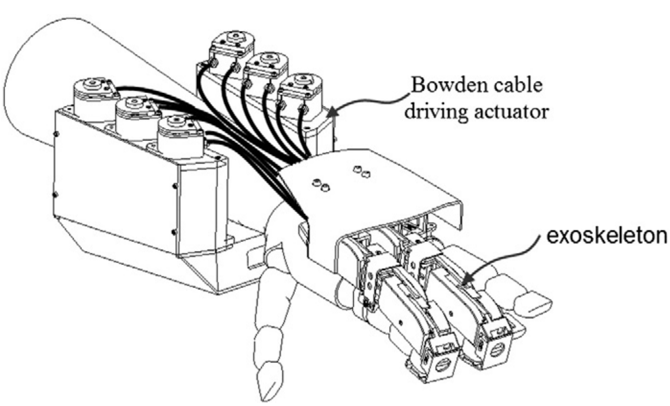

Fig. 1. Appearance of the hand exoskeleton for rehabilitation.

displacement S isn't suitable. The principle of rotating and stretching of the circuitous joint is shown in Fig. 3. In this way, the issue to accommodate to a variety of fingers is solved.

2.2. Optimal design of the circuitous joint

Since slide extension of the parallel mechanism is nonlinear, large slide extension will have a significant impact to the circuitous joint. In order to adapt to fingers of different sizes preferably and reduce the defects of the parallel mechanism, we made an optimization of structure parameters to pursue the goals as follows: make the virtual axis of the SPRM coincide with the axis of operator's phalanges as far as possible; the SPRM provides extension as much as possible and the parallel mechanism is just used to offset the shortage of the linear extension provided by the SPRM and to fulfill requirements of fingers of different sizes.

Seen in Fig. 4, the distance between the sliding pair and the centerline of the finger skeleton (d) is determined by the mechanical design and the thickness of the finger, so only the radius of the gear wheel (r) is adjustable.

Assume that two segments are fixed on the rings. The virtual axis V of the SPRM will not coincide with the axis C of operator's phalanges. The distance is p.

$$p = d - \frac{S}{\tan\frac{\theta}{2}} = d - r\frac{\theta}{\tan\frac{\theta}{2}} \tag{1}$$

The point V moves on the Y-axis by change of θ ($\theta \in \left[0, \frac{\pi}{2}\right]$) and its behavior is divided into three types according to the size of x (Fig. 5), where $r = xd$.

Considering its nearest trajectory to the point C, the preferable range of x is presumed as $0.5 \le x \le 2/\pi$, namely r is presumed as $0.5d \le x \le 2d/\pi$. The relation between the extension S_1 and θ is defined by the formula below and the optimal radius r should minimize it.

$$S_1 = d \times \tan\frac{\theta}{2} - S = d\left(\tan\frac{\theta}{2} - x\theta\right) \tag{2}$$

Fig. 6 shows the curves of the deviation S_1 vs. θ in several settings of the radius r. The radius r is set within the presumed range. To generalize the optimization, each parameter is dealt as a dimensionless number by dividing it by the offset d. Screening many curves and seeking a curve whose peak during a movable range of θ is minimum among them, the optimal r is found as the value that makes the sought curve. When the movable range is $0 \le \theta \le \pi/2$, the optimal radius r is 0.6d.

In the premise of fulfilling the adaptability, the most suitable r can be calculated by minimizing the absolute value of S_1 after setting an appropriate value of d. In this way, the structure parameters (shown in Table 1) of the three joint mechanisms optimized for the majority of normal adults can be obtained.

Based on the parameters optimized, the relation between the rotation angular displacement θ and the extension displacement is shown in Fig. 7. The shaded area represents extension displacement needed by different sizes of fingers. The solid line means the extension displacement provided by the SPRM and the area between two dash-dot lines indicates the sliding displacement of

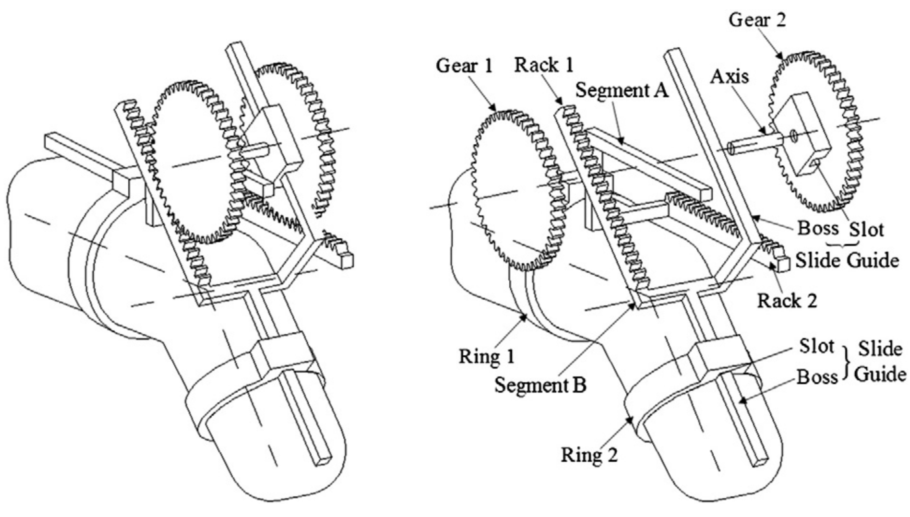

Fig. 2. Fundamental mechanism of the circuitous joint.

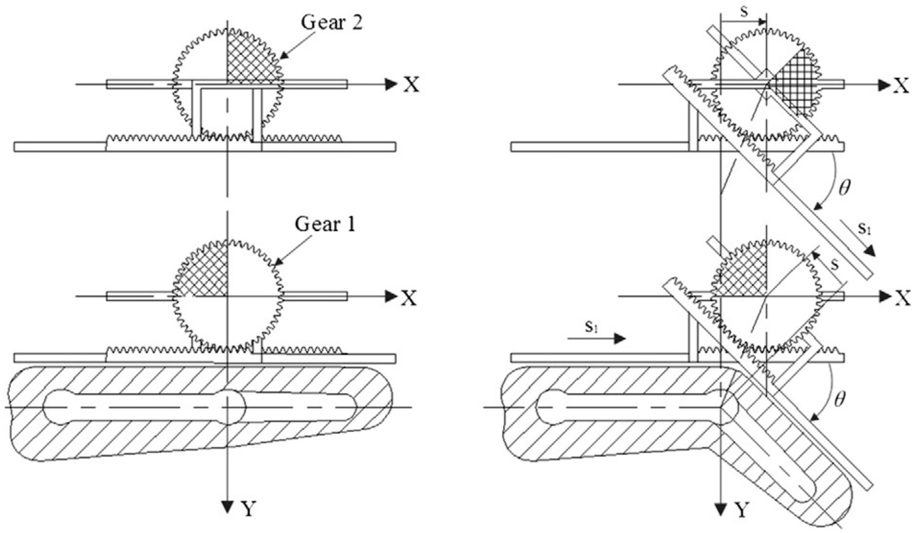

Fig. 3. Rotation and stretch of the circuitous joint. S is the stretching displacement produced by the SPRM and S_1 is the extra extension displacement obtained by the parallel sliding mechanism.

the parallel mechanism. We can see that this exoskeleton can adapt to different fingers and have a full range motion of bending and stretching.

2.3. Design of the hand exoskeleton

The circuitous joint assembly is shown in Fig. 8. In order to dissolve the interference between the mechanism and the operator's finger that has come up in the previous arrangements, the actual rack is placed on the opposite side viewed from the axis in comparison with the previous illustrations. The inverse gear is added to correct the stretching direction of each segment and carried on a slider to keep the position at the midpoint of the rack and the sector gear.

This exoskeleton consists of three circuitous joints in series corresponding to human finger's three joints (DIP, PIP, and MCP joint). The lengths of the fingers are different, so the lengths of the links are adjustable by changing the position of connecting screws. Additionally, in order to make the width small, the links overlap partly and alternately (Fig. 9). The width of the master finger is about 19[mm] which is the same as that of the humans. As shown in Fig. 10, this exoskeleton can adapt to the human finger in flexion and extension.

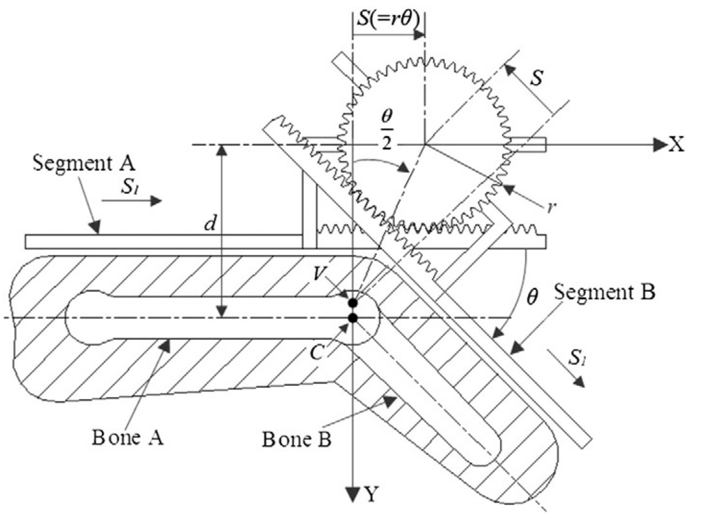

Fig. 4. Kinematical symbols in the circuitous joint.

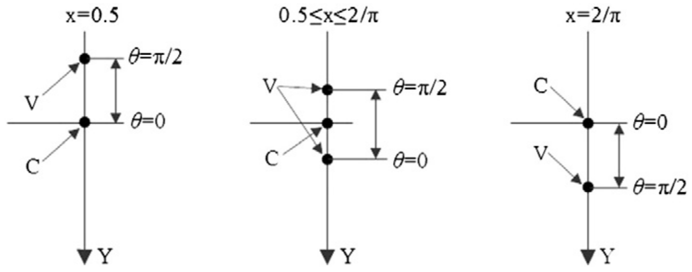

Fig. 5. Motion of the virtual axis V on the Y-axis by change of θ.

3. Driving and contact force analysis of the hand exoskeleton

3.1. Driving method of the hand exoskeleton

Bowden cable driving is adopted to actuate the exoskeleton. As shown in Fig. 11, each joint uses two cables and can be bilaterally driven. One end of each cable is twined on a winding drum which is driven by a motor and the other is twined on the pulley which is fastened on one of the inverse gears. Movement of the cable within the sheaths leads to a rotation of the pulley which results in a rotation of the finger's joint. Considering that cable transmission needs preload, adjustable screws are used. By adjusting the screws, the sheaths will be compressed to provide appropriate preload force.

The winding drums, motors and controller system are integrated in a driving box shown in Fig. 12 (designed for two exoskeletons). The driving box is placed on the forearm. This conception decreases the weight of the exoskeleton so as to reduce the burden on the finger.

3.2. Sensing and control

In order to realize hand rehabilitation, a general control system is designed, seen in Fig. 13. During a therapy, the patient is required to follow the indications of the training programs. Angular position sensors and force sensors are equipped to help realize the therapy. Position sensors have two roles in our rehabilitation robot: to realize position servo and to feed back the current joint position to the interactive training programs. Each DC motor is attached with a magnetic encoder (512 lines) and potentiometers (Zhongheng Electronics, Jason 1k) are installed on the shafts of the winding drums. Since the magnetic encoder is an incremental angle encoder, potentiometers are used to detect the absolute position. For collecting the force feedback and measuring the current joint positions, we place force sensors (Nitta Corporation, FlexiForce) in the contact areas between the exoskeleton and the fingers. The sensors are thin (0.125 mm) and light but have good linearity and sensitivity according to our experiment.

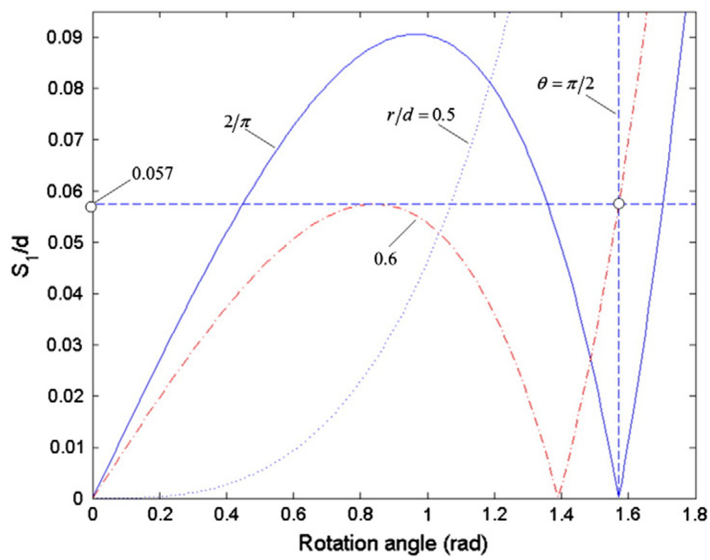

Fig. 6. Variation of the curves of the deviation S_1.

Table 1
Optimized structure parameters (mm).

Joint	θ	d	r	S_{max}	S_{1max}
MCP	0–90°	30–34	19.2	30.14	1.86
PIP	0–90°	25–27	15.6	24.49	1.51
DIP	0–80°	20–22	12.6	17.58	1.22

3.3. Contact force analysis of the hand exoskeleton

As a result of adopting the parallel mechanism, this exoskeleton can exert a force perpendicularly on the bone of the finger during the rehabilitation, which causes minimum secondary injuries. The analysis of the force orientation of the single circuitous joint is shown in Fig. 14.

The definitions of statics symbols are shown in Fig. 15.

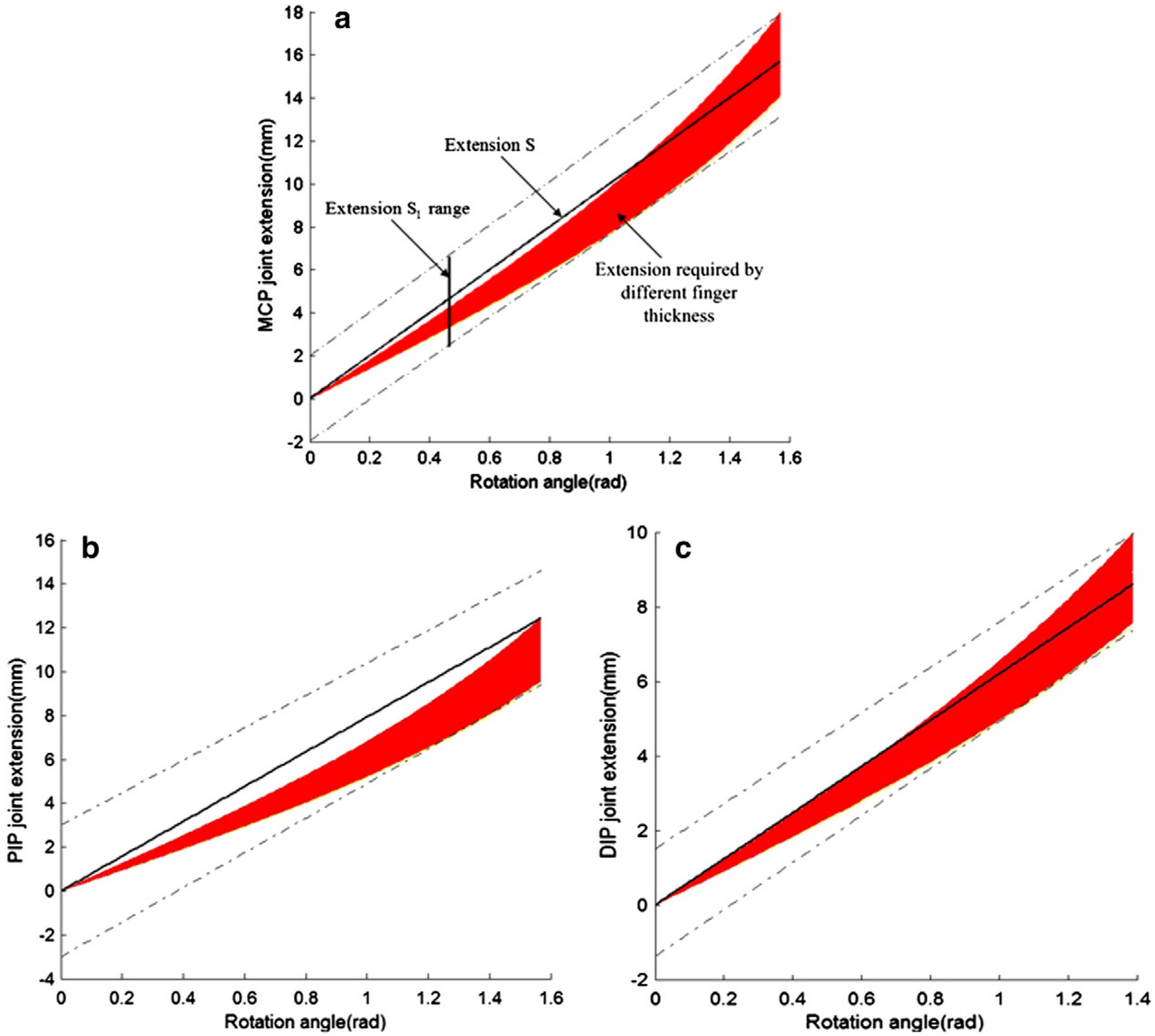

Fig. 7. Extension curves of the joints: (a) MCP, (b) PIP, (c) DIP.

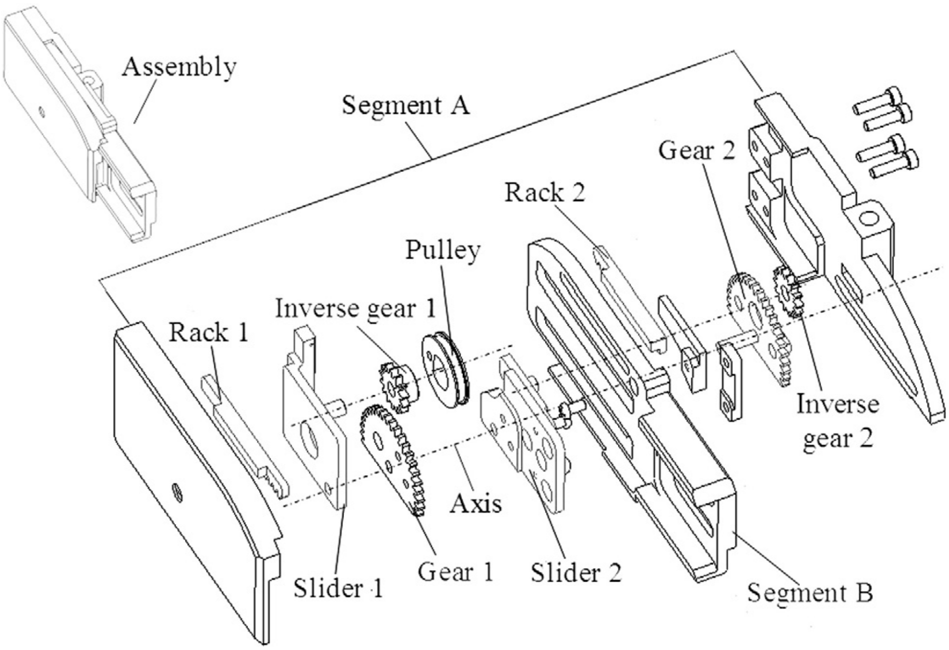

Fig. 8. The circuitous joint mechanism.

When the joint J_i has an angular displacement θ_i, the relation between the joint torque and the force applied perpendicularly to the bone of the finger is

$$\tau_i = \overrightarrow{J_i F} \times \overrightarrow{F_i} + \sum_{m=i}^{3} (\overrightarrow{J_i m_m} \times \overrightarrow{m_m G})(i = 1, 2, 3) \tag{3}$$

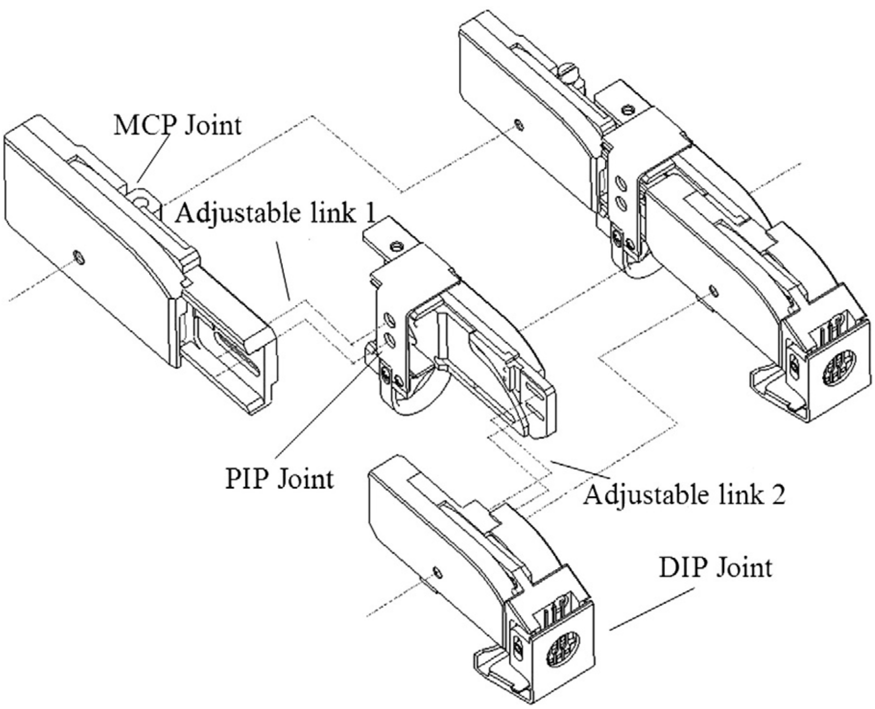

Fig. 9. The adjustable serial connection of the three joint units.

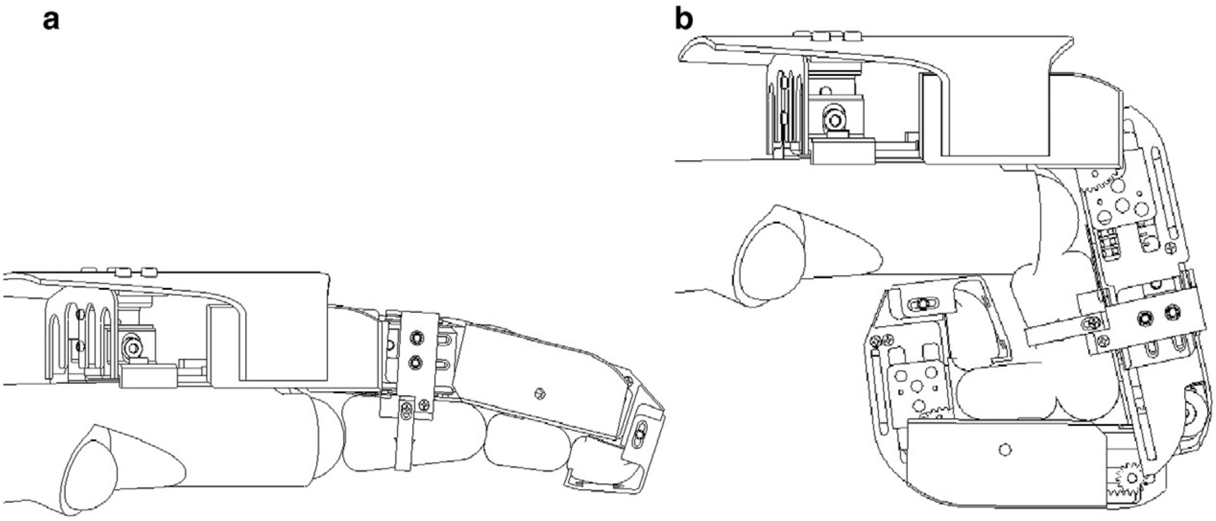

Fig. 10. Bending motion of the exoskeleton with three joints: (a) extension and (b) flexion.

where

$$\begin{cases} \overrightarrow{F_i} = F_i \begin{bmatrix} -\sin\theta_i \\ \cos\theta_i \end{bmatrix} \\ \overrightarrow{J_i F} = \left(b_i + \mathrm{d}_i \tan\dfrac{\theta_i}{2} \right) \begin{bmatrix} \cos\theta_i \\ \sin\theta_i \end{bmatrix} \\ \overrightarrow{m_i G} = m_i g \begin{bmatrix} 0 \\ 1 \end{bmatrix} \\ \overrightarrow{J_i m_i} = \left(a_i + \mathrm{d}_i \tan\dfrac{\theta_i}{2} \right) \begin{bmatrix} \cos\theta_i \\ \sin\theta_i \end{bmatrix} \end{cases} . \tag{4}$$

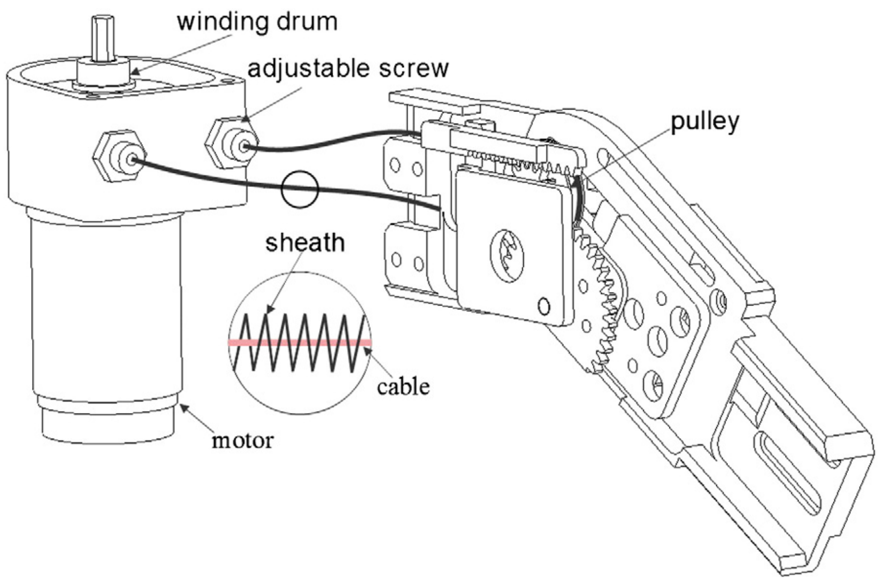

Fig. 11. Driving method of the exoskeleton.

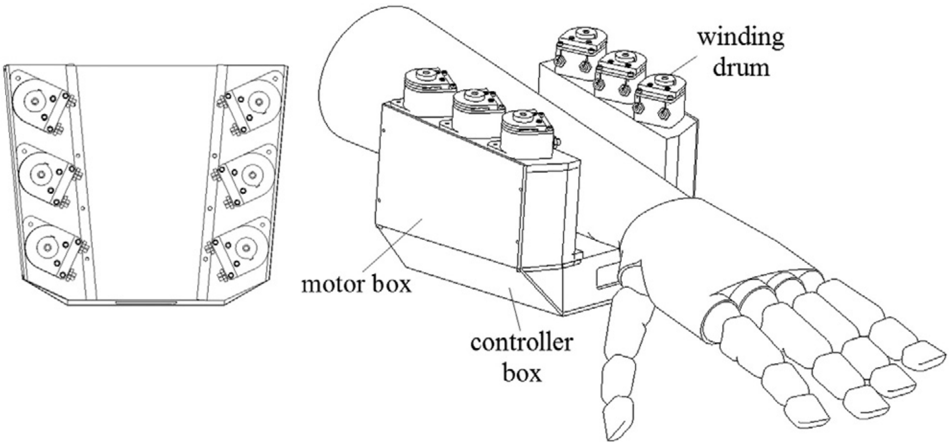

Fig. 12. Appearance of the driving box.

The sliding displacement of the parallel mechanism is very small, so if we ignore it, Eq. (3) is written as

$$\begin{cases} \tau_1 = F_1(b_1 + r_1\theta_1) + m_3 g(a_3 + r_3\theta_3)\cos\theta_3 + m_2 g(a_2 + r_2\theta_2)\cos\theta_2 + m_1 g(a_1 + r_1\theta_1)\cos\theta_1 \\ \tau_2 = F_2(b_2 + r_2\theta_2) + m_3 g(a_3 + r_3\theta_3)\cos\theta_3 + m_2 g(a_2 + r_2\theta_2)\cos\theta_2 \\ \tau_3 = F_3(b_3 + r_3\theta_3) + m_3 g(a_3 + r_3\theta_3)\cos\theta_3 \end{cases}. \quad (5)$$

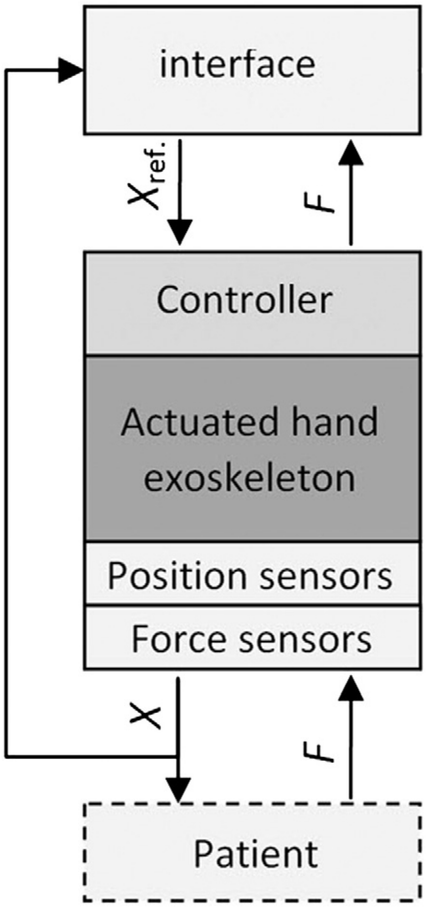

Fig. 13. Outline of the control system.

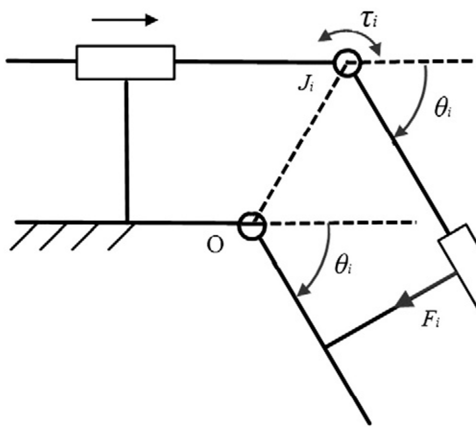

Fig. 14. Analysis of the force orientation.

Thus, the relation among the joint angular displacement θ_i, the force F_i and the torque τ_i is obtained.

4. Experiment

4.1. Hand fitness test

One of the important aspects for evaluation of the rehabilitation exoskeleton is the ability to adapt to different fingers. Our exoskeleton based on the circuitous joint can adapt to different radiuses of fingers and the length of the exoskeleton is adjustable by changing the position of the connecting screws. Fig. 16 shows the hand fitness experiment. We can see that the same exoskeleton can adapt to fingers of different subjects.

4.2. Contact force analysis experiment

To confirm the contact force analysis between the exoskeleton and the finger mentioned above, a control experiment is conducted. The experiment is shown in Fig. 17.

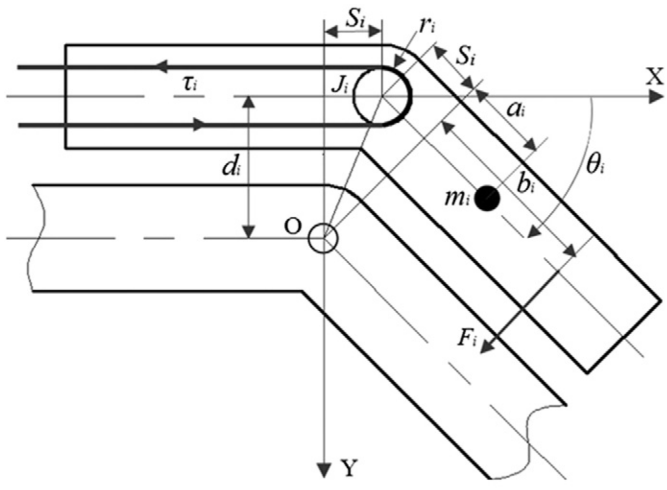

Fig. 15. Force equilibrium on the joint. J_i: Joint number; d_i: Distance between the virtual axis of the SPRM and the axis of phalanges; S_i: Joint stretching displacement; θ_i: Joint angular displacement; r_i: Radius of the sector gear; τ_i: Joint torque; F_i: Force applied perpendicular to the bone of the finger; m_i: Weight of the joint; a_i: Distance between the center of mass of the joint and the axis; b_i: Distance between the origin of the force and the axis.

Experiments are carried out on each joint of a finger. The motor torque is given as shown in Fig. 18. We compared the motor torque generated by PID control and the theoretical one calculated by Eq. (5). The theoretical motor torque is calculated using the following parameters,

$$\begin{cases} m_1 = 0.0853(\mathrm{kg}), m_2 = 0.0651(\mathrm{kg}), m_3 = 0.0548(\mathrm{kg}) \\ a_1 = 0.0102(\mathrm{m}), a_2 = 0.0087(\mathrm{m}), a_3 = 0.0076(\mathrm{m}) \\ b_1 = 0.045(\mathrm{m}), b_2 = 0.025(\mathrm{m}), b_3 = 0.02(\mathrm{m}) \\ \mathrm{r}_1 = 0.0192(\mathrm{m}), \mathrm{r}_2 = 0.0156(\mathrm{m}), \mathrm{r}_3 = 0.0126(\mathrm{m}) \end{cases}. \tag{6}$$

The result is shown in Fig. 19. The horizontal axis represents the joint rotation angular displacement and the vertical axis represents the contact force. During the experiment we collected some discrete force values. An obvious accordance of real and theoretical values can be seen. Thus, the analysis mentioned above can be verified. Since the contact force is obtained based on the assumption that the force is perpendicular to the finger. The experiment results also denote that the exoskeleton is suitable for medical application and causes minimum secondary injuries.

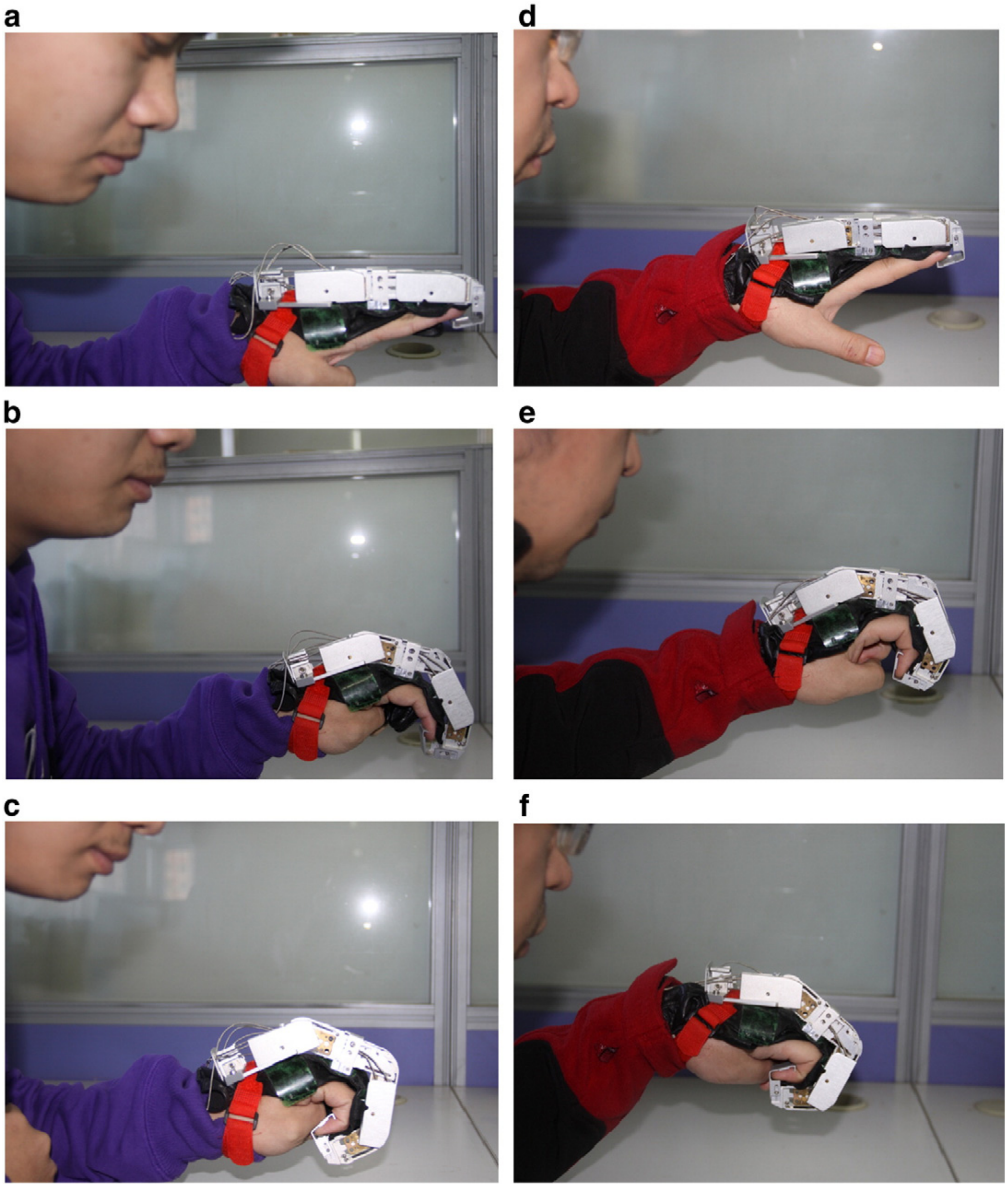

Fig. 16. Hand fitness test: (a), (b), and (c): hand fitness test of the first conner; (d), (e), and (f): hand fitness test of the second conner.

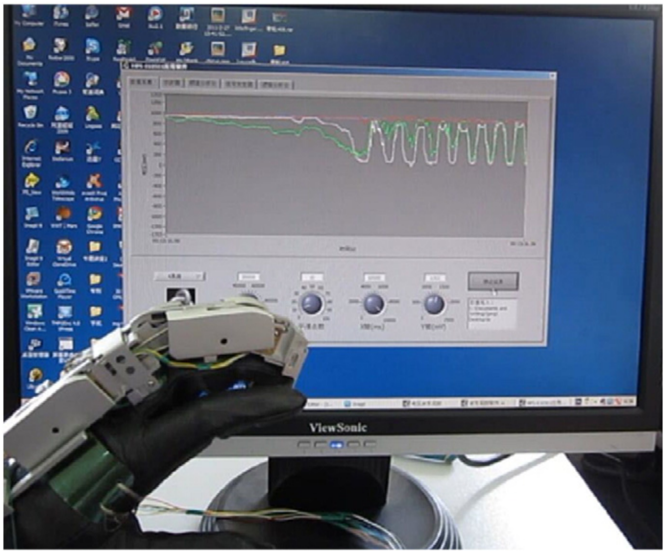

Fig. 17. Contact force analysis experiment.

5. Conclusion

Focusing on adapting to fingers of different sizes and avoiding secondary injuries, a novel hand exoskeleton device including the adaptive exoskeleton and the Bowden cable driving actuator is proposed. Adopting proposed circuitous joints composed of the SPRM and the parallel sliding mechanism can realize the non-linear stretching displacement of the joint to cover wide workspace of the finger and ensure the force exerted by the exoskeleton perpendicular to the bone of the finger. The Bowden cable driving method places the driving and control system on the forearm. This conception reduces the burden on the fingers. The results of the hand fitness test and the contact force experiment verify the rationality and effectiveness of the exoskeleton.

Acknowledgments

We would like to thank Dr. M. B. Piao and Mr. S. B. Yan for their valuable suggestion on the paper. This work is supported in part by the National Natural Science Foundation of China (Grant No. 61203347), the Fundamental Research Funds for the Central Universities (Grant No. HIT. NSRIF. 2013047), and the China Postdoctoral Science Foundation (Grant No. 2013M531023).

Appendix A. Supplementary data

Supplementary data to this article can be found online at http://dx.doi.org/10.1016/j.mechmachtheory.2013.10.015.

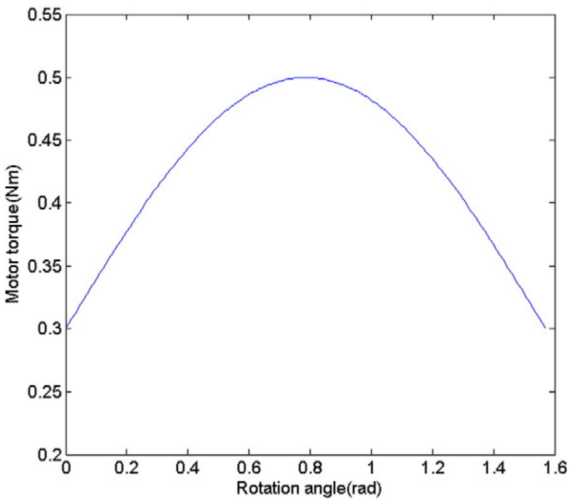

Fig. 18. Motor torque curve.

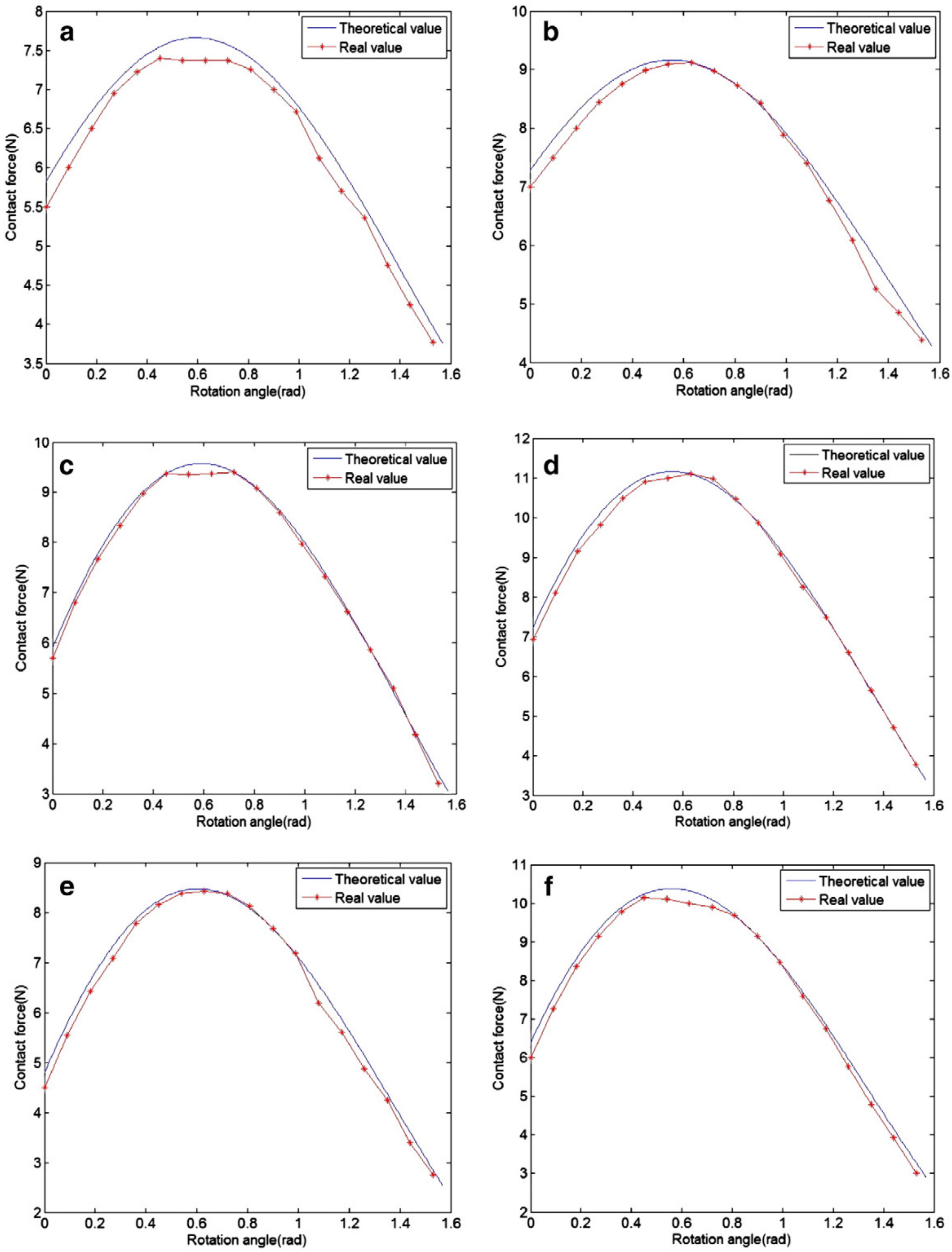

Fig. 19. Relation between real values and theoretical ones: (a) MCP joint, (b) PIP joint ($\theta_3 = 0$), (c) PIP joint ($\theta_3 = 90°$), (d) DIP joint ($\theta_3 = 0$, $\theta_2 = 0$), (e) DIP joint ($\theta_3 = 90°$, $\theta_2 = 0$), and (f) DIP joint ($\theta_3 = 90°$, $\theta_2 = 90°$).

References

[1] S.W. O'Driscoll, N.J. Giori, Continuous passive motion (CPM): theory and principles of clinical application, J. Rehabil. Res. Dev. 37 (2) (2000) 179–188.
[2] H.C. Fischer, K. Stubblefield, T. Kline, X. Luo, R.V. Kenyon, D.G. Kamper, Hand rehabilitation following stroke: a pilot study of assisted finger extension training in a virtual environment, Top. Stroke Rehabil. 14 (1) (2007) 1–12.

[3] H.G. Fang, Z.W. Xie, H. Liu, An exoskeleton master hand for controlling DLR/HIT hand, Proceedings of the IEEE/RSJ International Conference on Intelligent Robots and Systems, St. Louis, 2009, pp. 3703–3708.
[4] N. Shuhei, K. Hiroyuki, K. Naoki, T. Susumu, K. Ichiro, An encounter-type multi-fingered master hand using circuitous joints, Proceedings of the IEEE International Conference on Robotics and Automation, Barcelona, 2005, pp. 2667–2672.
[5] H.G. Fang, Z.W. Xie, H. Liu, T. Lan, J.J. Xia, An exoskeleton force feedback master finger distinguishing contact and non-contact mode, Proceedings of the IEEE/ASME International Conference on Advanced Intelligent Mechatronics, Singapore, 2009, pp. 1059–1064.
[6] M. Bouzit, G. Burdea, G. Popescu, R. Boian, The Rutgers Master II — new design force-feedback glove, IEEE/AMSE Trans. Mechatron. 7 (2) (2002) 256–263.
[7] W. Andreas, K. Konstantin, H. Günter, R. Boian, Mechanical design and motion control of a hand exoskeleton for rehabilitation, Proceedings of the IEEE International Conference on Mechatronics and Automation, Niagara Falls, 2005, pp. 155–159.
[8] W. Andreas, H. Günter, Development and control of a hand exoskeleton for rehabilitation of hand injuries, Proceedings of the IEEE/RSJ International Conference on Intelligent Robots and Systems, Alberta, 2005, pp. 3046–3051.
[9] T.T. Worsnopp, M.A. Peshkin, J.E. Colgate, D.G. Kamper, An actuated finger exoskeleton for hand rehabilitation following stroke, Proceedings of the IEEE 10th International Conference on Rehabilitation Robotics, Noordwijk, 2007, pp. 896–901.
[10] H. Yamaura, K. Matsushita, R. Kato, H. Yokoi, Development of hand rehabilitation system for paralysis patient-universal design using wire-driven mechanism, Proceedings of the 31th Annual International conference of the IEEE EMBS, Minnesota, 2009, pp. 7122–7125.
[11] Y.L. Fu, P. Wang, S.G. Wang, H.S. Liu, F.X. Zhang, Design and development of a portable exoskeleton based CPM machine for rehabilitation of hand injuries, Proceedings of the IEEE International Conference on Robotics and Biomimetics, Sanya, 2007, pp. 1476–1481.
[12] S. Wang, J.T. Li, R.Y. Zheng, Z.Y. Chen, Y.R. Zhang, Multiple rehabilitation motion control for hand with an exoskeleton, Proceedings of the IEEE International Conference on Robotics and Automation, Shanghai, 2011, pp. 3676–3681.
[13] J.T. Li, S. Wang, J. Wang, R.Y. Zheng, Y.R. Zhang, Z.Y. Chen, Development of a hand exoskeleton system for index finger rehabilitation, Chin. J. Mech. Eng. 25 (2) (2012) 223–233.
[14] Y.L. Fu, Q.C. Zhang, F.H. Zhang, Z.K. Gan, Design and development of a hand rehabilitation robot for patient-cooperative therapy following stroke, Proceedings of the IEEE International Conference on Mechatronics and Automation, Beijing, 2011, pp. 112–117.
[15] S.V. Adamovich, A.S. Merians, R. Boian, M. Tremaine, G.S. Burdea, M. Recce, H. Poizner, A virtual reality based exercise system for hand rehabilitation post-stroke: transfer to function, Proceedings of the 26th Annual International Conference of the IEEE EMBS, San Francisco, 2004, pp. 4936–4939.
[16] M.J. Lelieveld, T. Maeno, Design and development of a 4 DOF portable haptic interface with multi-point passive force feedback for the index finger, Proceedings of the IEEE International Conference on Robotics Automation, Orlando, 2006, pp. 3134–3139.